

## Article

# Intermediate Pyrolysis of Brewer's Spent Grain: Impact of Gas Atmosphere

Artur Bieniek <sup>1,\*</sup>, Wojciech Jerzak <sup>1</sup>, Małgorzata Sieradzka <sup>1</sup>, Łukasz Mika <sup>2</sup>, Karol Sztékler <sup>2</sup>  
and Aneta Magdziarz <sup>1</sup>

<sup>1</sup> Faculty of Metals Engineering and Industrial Computer Science, AGH University of Science and Technology, Al. Mickiewicza 30, 30-059 Cracow, Poland; wjerzak@agh.edu.pl (W.J.); msieradz@agh.edu.pl (M.S.); amagdzia@agh.edu.pl (A.M.)

<sup>2</sup> Faculty of Energy and Fuels, AGH University of Science and Technology, Al. Mickiewicza 30, 30-059 Cracow, Poland; lmika@agh.edu.pl (Ł.M.); sztekler@agh.edu.pl (K.S.)

\* Correspondence: artbie@agh.edu.pl

**Abstract:** This work focuses on the impact of carrier gas on the quantity and quality of pyrolytic products received from intermediate pyrolysis of the brewer's spent grain. In this study, three types of carrier gases were tested: argon, nitrogen, and carbon dioxide at three temperatures of 500, 600, and 700 °C. On the basis of the process conditions, the yield of products was determined. The ultimate analysis of the char was performed, and for selected chars, the combustion properties were determined. Gas chromatography of the organic fraction of oil was performed, and the compounds were determined. Additionally, microscale investigation of the spent grain pyrolysis was performed by thermogravimetric analysis. The results showed that there were no significant differences in product yields in various atmospheres. Char yield changed only with temperature from 28% at 500 °C up to 19% at 700 °C. According to ultimate analysis, the char from CO<sub>2</sub> pyrolysis was approximately 2% richer in carbon and this fact did not influence on the combustion properties of the char. The oil fraction was characterized mainly by acids with a maximum content of 68% at 600 °C in an argon atmosphere and the acid concentration depended on the carrier gas as follows line: Ar > N<sub>2</sub> > CO<sub>2</sub>.

**Keywords:** Brewer's spent grain; intermediate pyrolysis; carrier gas; fixed bed reactor



**Citation:** Bieniek, A.; Jerzak, W.; Sieradzka, M.; Mika, Ł.; Sztékler, K.; Magdziarz, A. Intermediate Pyrolysis of Brewer's Spent Grain: Impact of Gas Atmosphere. *Energies* **2022**, *15*, 2491. <https://doi.org/10.3390/en15072491>

Academic Editor: Changkook Ryu

Received: 28 February 2022

Accepted: 25 March 2022

Published: 28 March 2022

**Publisher's Note:** MDPI stays neutral with regard to jurisdictional claims in published maps and institutional affiliations.



**Copyright:** © 2022 by the authors. Licensee MDPI, Basel, Switzerland. This article is an open access article distributed under the terms and conditions of the Creative Commons Attribution (CC BY) license (<https://creativecommons.org/licenses/by/4.0/>).

## 1. Introduction

Current energy and ecological policy promotes the reuse and management of all types of municipal and industrial solid wastes in technological processes [1,2]. The main goal of this promotion is to reduce the amount of waste in landfills and also search for alternative solutions for fossil fuels. The use of municipal solid waste in the power engineering sector allows a reduction the amount of fossil fuels involved in energetic processes. Especially organic wastes are worth considering. This is important because fossil fuels have limited resources and can be regenerated over long periods of time [3,4]. Another reason is the fact that global demand for primary energy is dynamically increasing, and it leads to intensified consumption of all kinds of fuel, especially fossil fuels such as natural gas, coal, or oil [5].

In 2000, the usage of industrial and municipal solid waste in the energy sector allowed to produce approximately 1.24 EJ of primary energy, and in 2019, the production of primary energy from waste was 2.59 EJ [6]. It was above two times the increase in waste share in the primary energy generation structure. Most wastes are characterized by an organic chemical structure, and these wastes can be classified as biomass sources, according to the definition of biomass included in the directive of the European Parliament and of the Council [7]. Biomass as a source of energy belongs to renewable energy sources. From this point of view, the reuse of waste in the energy process has a lot of energetic, economical, and ecological benefits [8].

Today, the power engineering sector uses organic wastes primarily in combustion, where the chemical energy is converted to heat that could be used in other processes [9–11]. Another method is the thermal conversion of solid waste into valuable fuels by a process such as pyrolysis. The primary feedstock is thermally degraded in the absence of an oxygen atmosphere, where, in the results, long polymer structures are broken into smaller chemical compounds. This process is called pyrolysis and usually operates in the temperature range of 350 °C to 750 °C [12–14]. Pyrolysis always delivers three types of products: solid residue, condensable fraction of heavy hydrocarbons, and light-weight gases. Solid residues are built with fixed carbon and ash included in feedstock, while volatile matter and noncondensable gases are gaseous products of the degradation of long structure of polymers.

An example of food industrial solid waste is brewer's spent grain (BSG). Brewer's spent grain is organic residue generated after the beer production process. In 2020, around 32 billion L of beer were produced in the European Union [15]. Production of 100 L of beer was estimated to require 20–22 kg of barley malt, which is the primary organic component [16]. According to the presented data, it can be observed that a large amount of BSG could be obtained and reused in the energy sector. Nowadays, BSG waste is converted to animal feed due to high content of nutrients, even after the brewing process, or is stored in landfills [16,17].

BSG as a waste material could be involved in the power engineering sector. Because of its organic nature, it is classified as a biomass, and its use could increase the impact of green energy on the structure of primary energy demand. The wet BSG waste directly from the lauter tun contains around 77–81% water, and for further processes, the BSG should be dried to increase its energetic potential [18,19]. BSG is considered as fuel in the combustion process where the included chemical energy is transformed into heat [20,21]. It is characterized by a higher calorific value of 17.8 up to 19.1 MJ·kg<sup>-1</sup> and a relatively small ash content of 1.7% to 5.4% [22]. On the other hand, many scientific works present BSG as a good example of feedstock material in pyrolysis or other chemical processes of solid material conversion [23–27]. Because of these methods, valuable chemical compounds can be evolved from BSG. Čater et al. [23] investigate a method of to produce biogas from brewer's spent grain by bioaugmentation enhanced with anaerobic hydrolytic bacteria. The results of the researchers have shown that 17.8% of the methane from BSG can be produced with the bioaugmentation of pseudobutyrvibrio xylanivorans. Yinxin et al. [24] investigated a co-pyrolysis of BSG and sewage sludge in a limited oxygen atmosphere (<5%). The results have shown that the higher the content of sewage sludge in the primary mixture, the higher the pH and the lower the ash content in the biochar received. The conversion of BSG to calorific fuel has been reported in [25], where intermediate pyrolysis combined with catalytic steam reforming was investigated by Mahmood et al. That research has shown that higher temperature affects gaseous product production, and the heating value of gas was from 10.8 to 25.2 MJ/m<sup>3</sup>, depending on the conditions. The microscale of BSG pyrolysis was described by Borel et al. [26]. Researchers used thermogravimetry analysis to investigate the thermal degradation of a BSG in the presence of nitrogen atmosphere. On the basis of the curves received from the TG analysis, scientists evaluated the independent parallel reaction model of the pyrolysis of basic components of BSG.

This paper provides a study of the intermediate pyrolysis of the brewer's spent grain in a laboratory scale fixed-bed reactor. This work focuses mainly on the impact of a gaseous atmosphere on the pyrolysis process. Based on the literature review, it was found that only some investigations presented the influence of sweeping gas on different types of pyrolysis, mainly in fast pyrolysis, with diversified biomass feedstocks [28–31]. Thus, the main goal of this paper was to compare the quality and quantity of products obtained under three kinds of atmosphere (Ar, N<sub>2</sub>, and CO<sub>2</sub>). In [28], Zhang et al. investigated a fast pyrolysis of corncob in a fluidized reactor under five different carrier gases: nitrogen, carbon dioxide, carbon monoxide, methane, and hydrogen. The results suggested that the smallest amount of bio-oil would be obtained under the CO atmosphere, and it was 49.6%, while the other gases gave similar results, and the liquid fraction was around

58%. Similar experiments were carried out by Liu et al. [29]. Researchers investigated the pyrolysis process of binder cold-briquetted lignite (BCBL) in a fixed bed reactor under carbon monoxide, carbon dioxide, methane, hydrogen, and nitrogen atmosphere. Scientists received the specific surface area of semichars in the range of 1.71–2.53 m<sup>2</sup>/g where the lowest value was received for the CO atmosphere and the highest for N<sub>2</sub>. Investigation of the impact of gaseous atmosphere on the pyrolysis process could also be found in [30], where Zhang and Zhang conducted experiments concerning a catalytic microwave-induced fast pyrolysis of medicinal herb residue under carbon dioxide, carbon monoxide, hydrogen, and nitrogen, and their studies were focused on determining the pyrolytic product yields and oil chemical compositions. The received results showed the dependency between the maximum content of the oil fraction and the gas atmosphere in the following line N<sub>2</sub> > CO<sub>2</sub> > H<sub>2</sub> > CO. These results confirm the results of the work [28].

In this work, studies concerning the impact of the gaseous atmosphere on the pyrolytic products from intermediate pyrolysis have been presented. This article focuses on the quality and quantity analysis of the pyrolytic products received under various conditions. The aim of this article was to provide an answer to the following questions: Are there crucial differences in the quality of products obtained under different gases in intermediate pyrolysis? Is it possible to reduce the amount of N-containing compounds in the oil if commonly used nitrogen is replaced by argon?

Moreover, intermediate pyrolysis compared to fast and slow pyrolysis characterizes the same yields of char, gas, and oil. This distribution of yields is desirable in the production process. As reported in the newest paper [32] that intermediate pyrolysis with polygeneration may play important role in the reduction of CO<sub>2</sub> emissions up to 2050. The additional advantage of intermediate pyrolysis is the fact that oil has less oxygen content than that from fast pyrolysis. Moreover, the feedstocks used in intermediate pyrolysis can contain significant amounts of moisture, and hence, they do not require a pretreatment process. Thus, the motivation of this work was the investigation of the impact of carrier gas on intermediate pyrolysis. This fact makes this study novel, and the presented results may enhance the knowledge about another kind of pyrolysis.

## 2. Materials and Methods

The experiments were carried out in a horizontal fixed-bed reactor with a nonlinear heating rate of the sample. Three different carrier gases were selected: argon and nitrogen, which are considered non-reactive gases with solid feedstock, and carbon dioxide, which at higher temperatures could react with carbon [33]. The tests were carried out at three temperatures of 500, 600, and 700 °C to determine the effect of temperature on the received results.

Pyrolytic products were divided into three groups: solid residue (char), condensable fraction (oil), and light-weight gases. For every investigated case, the yield of products was determined. Chars were analyzed via ultimate analysis, and carbon, nitrogen, and hydrogen contents were determined. For selected chars obtained under a nitrogen and carbon dioxide atmosphere, combustion characteristics were plotted, and ignition and burnout temperatures were determined. The organic fraction of oil was analyzed by gas chromatography technique. Organic compounds which form the structure of oil have been determined and classified into chemical groups. Furthermore, the main experiments have been supplied by the microscale study involving a thermogravimetric analysis, where the pyrolysis behavior of BSG under considered gases was recorded.

### 2.1. Characterization of Feedstock

Brewer's spent grain (BSG) was selected as a feedstock material. This feedstock is the main organic residue after the beer production process. The BSG for the tests was supplied from the Polish brewery industry located in AGH Cracow. The material was collected directly after the brewing process, and the feedstock was immediately packed in hermetic bags and stored at 4 °C to prevent microbial fermentation during delivery. The

raw feedstock contained a lot of moisture and for this reason, the BSG was dried at 40 °C for several days. Then, the air-dried material was milled, and for further experiments, nonuniform size particles (less than 1 mm) were selected. It was expected that the non-uniform size of the particles would be characterized by a lower bulk density. Consequently, the biomass sample should have more spaces to release volatile matter, and carrier gas should have easier sweeping into the sample.

## 2.2. Experimental Setup

Intermediate pyrolysis experiments of the brewer's spent grain were carried out in a horizontal fixed bed reactor. The reactor scheme is presented in Figure 1.

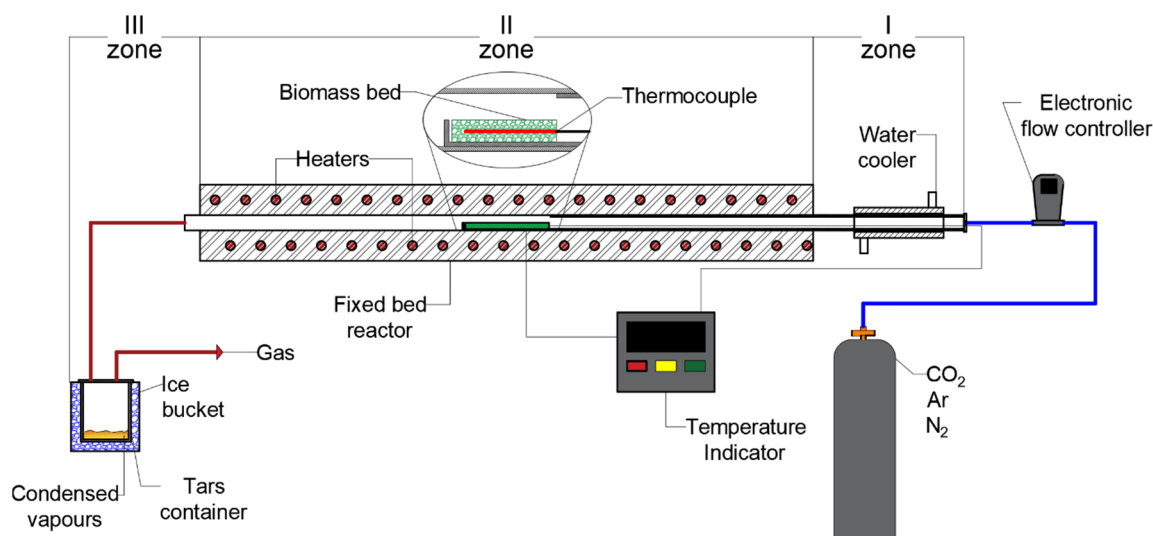


**Figure 1.** Experimental setup for the intermediate pyrolysis process.

The fixed-bed reactor is built with two concentric positioned stainless-steel pipes: external and internal. The external pipe is motionless and is surrounded by electric heaters. The external pipe with the heaters is enclosed by ceramic insulation. The internal pipe is placed inside the external pipe, and this pipe is able to move by push. In the internal pipe, a longitudinal hole was created, and in this hole, the feedstock was placed. The biomass sample was inserted into the reactor when the internal pipe was pushed.

The presented laboratory setup consists of three main sections. In the first zone, on the right side of Figure 1, a biomass sample was prepared for the experiment, and the solid residues were cooled after pyrolysis. BSG sample (1 g) was applied to the reactor. The sample was pyrolyzed for 3 min, and after this time, the sample was cooled. Inside the internal pipe, the sweeping gas was flowing. Nitrogen, argon, and carbon dioxide were chosen, and for each case, the volume flow rate was set at 300 mL/min. The purity of each gas was 99.9999%. The flow rate was monitored by an electronic regulator. Additionally, in a first zone, the water cooler was installed which allowed to cool a solid residue after pyrolysis.

In the second zone, the fixed-bed reactor was placed where intermediate pyrolysis was conducted. Heat was supplied by electrical heaters. The reactor temperature was measured on the wall of the external pipe using a K thermocouple. In this study, the temperature was set at 500 °C, 600 °C, and 700 °C.

The temperature was controlled by an autotransformer, and the temperature value was displayed in the indicator. During the experiment, in the initial time, a temperature drop of approximately 30–40 °C was observed due to the insertion of a cold internal pipe with the sample. Then, the temperature returned to the initial temperature. In this laboratory setup, cold feedstock was inserted into the preheated reactor up to the set temperature of the process, and the sample was heated with the non-linear heating curve. The detailed description of the non-linear heating rate can be found in previous research [34].

The last part of the setup provided the capture of liquid and gaseous products. Water and heavy hydrocarbons from volatile matter were liquified in a container that had been placed in an ice bucket. The remaining gases left the reactor and were not captured for analysis.

### 2.3. Analytical Methods of Feedstock and Products Characterization

#### 2.3.1. Ultimate, Proximate, and Fiber Analysis

The elemental composition of brewer's spent was determined using a Truspec CHNS 628 Leco analyzer. All solid products from intermediate pyrolysis of BSG under considered gaseous atmospheres were also analyzed by ultimate analysis involving the same device. This apparatus determines carbon, hydrogen, and nitrogen content using combustion methods. A pre-weighted sample was inserted to the furnace where it was combusted with pure oxygen to carbon dioxide (CO<sub>2</sub>) and steam (H<sub>2</sub>O). High temperatures also allowed to create NO<sub>x</sub>. The species received on detectors determine the content of basic elements.

Proximate analysis was performed for air-dried brewer's spent grain only. Moisture, volatile matter and ash content were determined according to the standards EN ISO 18134-2:2017, EN ISO 18122:2015, and EN ISO 18122:2015, respectively.

Fiber structure analysis of BSG was conducted according to van Soest method [35] to enhance knowledge about cellulose, hemicellulose, and lignin content. All basic analyzes of feedstock properties were duplicated.

#### 2.3.2. Thermogravimetric Analysis

Thermogravimetric analysis was involved to investigate the impact of carrier gas on the BSG pyrolysis and also to determine the combustion properties of selected chars.

The mass loss of the BSG under the respected gases was determined using a STA 449 F3 Jupiter thermal analyzer. Approximately 12 mg of the sample was loaded onto platinum crucibles with an Al<sub>2</sub>O<sub>3</sub> inlay. The sample was heated from ambient temperature to 800 °C at a heating rate of 5 K/min with a volume flow rate of 70 mL/min. After reaching the final temperature, the sample was kept for 20 min under isothermal conditions. Then, it was cooled to the initial temperature again.

According to the results of ultimate analysis of solid residues from intermediate pyrolysis, the chars received under carbon dioxide and nitrogen atmosphere at the lowest and the highest temperatures were selected for thermogravimetry analysis. The reason for choosing only four cases for TG analysis was as an attempt to investigate the char received under one of the inert atmospheres and compare it to the char from the reactive atmosphere at a given temperature.

These experiments were performed using Mettler Toledo TGA/SDTA 851. Around 6 mg of char was placed in a corundum crucible. The sample was then combusted under air atmosphere with a volume flow rate of 40 mL/min. The char was heated at a heating rate of 10 K/min from ambient temperature to 800 °C. During the experiments, mass loss, time, and temperature were recorded, and combustion profiles were determined. The results of the TG analysis, and their graphical interpretation allowed the ignition temperature and the burnout temperature to be found [36].

The ignition temperature refers to the minimum temperatures at which fuels spontaneously ignite without external source of ignition. The ignition temperature was determined according to work [36]. The burnout temperature is the temperature at which 99% of the initial fuel mass was converted.

All experiments were performed twice to test the repeatability, and a good consistency, with the standard errors of  $\pm 1$  °C, was observed.

#### 2.3.3. Products Yield

The products from intermediate pyrolysis were classified into three main groups: char (solid residue), oil fraction, (liquid fraction consisted with organic fraction of condensable

vapors and water), and non-condensable gases. The yield of each pyrolysis product was computed according to Equations (1)–(3).

$$Y_{char} = \frac{M_{char}}{M_{biomass}} \cdot 100\% \quad (1)$$

$$Y_{oil} = \frac{M_{oil}}{M_{biomass}} \cdot 100\% \quad (2)$$

$$Y_{gas} = 100\% - Y_{oil} - Y_{char} \quad (3)$$

where  $Y_x$  is the yield of  $x$  and  $M_x$  refers to the mass of  $x$ .

#### 2.3.4. Gas Chromatography–Mass Spectroscopy

The liquid fraction collected from the intermediate pyrolysis contained a condensable fraction of volatiles (tar) and water. For further investigations, water had been separated, and only the organic fraction was analyzed. The purpose of the tar analysis was to identify the quality and quantity of the compound that built the oil structure received under various conditions. Analysis was performed using gas chromatography mass spectroscopy (GC–MS) and an Agilent GC 7890 B apparatus equipped with an MS 5977A mass spectrometer and a flame ionizer detector. Before analysis, the tars were dissolved in acetone. Then, tar analysis was carried out according to the evaporation of compounds from the samples. The sample was heated from 40 to 300 °C at a rate of 3 °C/min and kept for 10 min. The relative content of the determined compound was calculated as a ratio of the peak area of the compound to the sum of all the compound areas of the peak detected. All samples were investigated two times.

### 3. Results

#### 3.1. Brewer's Spent Grain Properties

The results of the ultimate, proximate, and component analysis of BSG are presented in Table 1. An air-dry brewer's spent grain lost approximately 70% of the water that was included in the as-received state [18]. BSG contains a large amount of volatiles, and this fact classifies it as a good candidate for pyrolysis, especially for oil production, where large amount of volatiles is desirable.

**Table 1.** Results of ultimate, proximate, and component analysis of BSG in an air-dry state.

Ultimate Analysis (wt%)	
C	47.57
H	6.78
N	4.08
<sup>a</sup> O	41.59
Proximate Analysis (wt%)	
Moisture (M)	6.23
Volatile matter (VM)	81.57
Ash (A)	3.35
<sup>b</sup> Fixed carbon (FC)	8.85
Component Analysis (wt%)	
Cellulose	17.18
Hemicellulose	34.16
Lignin	3.12
Extractives	45.54

<sup>a</sup> O: by difference, ash free. <sup>b</sup> FC = 100 wt%–M–VM–A.

The BSG is built mainly from extractives such as proteins, fats, and sugars. Lignocellulosic hardwood feedstock is mainly composed of three main components, lignin, cellulose, and hemicellulose, and cellulose is the main component. In the case of agricultural biomass such as BSG, extractives constitute the main substances. It means that BSG is still rich in nutrients and, for this reason, is reused for animal food.. The results proved that lignin has the lowest share as a component, which is the main contributor in char formation during pyrolysis [37]. Additionally, fixed carbon is only 8.85%, and these facts lead to less char production than in the case of hardwood feedstocks [38]. The results of BSG characterization are compatible with data from the literature review [25,39].

### 3.2. Results of Thermogravimetry Analysis of BSG

The impact of carrier gas on the pyrolysis process was also tested on a microscale involving thermogravimetric analysis. The main goal was to determine the conversion behavior of the feedstock during heating under respectable gases. The thermogravimetric curves for BSG pyrolysis under  $N_2$ ,  $CO_2$ , and Ar atmospheres are presented in Figure 2. Based on TG analysis, the derivative thermogravimetric (DTG) curves were created and are presented in Figure 2.

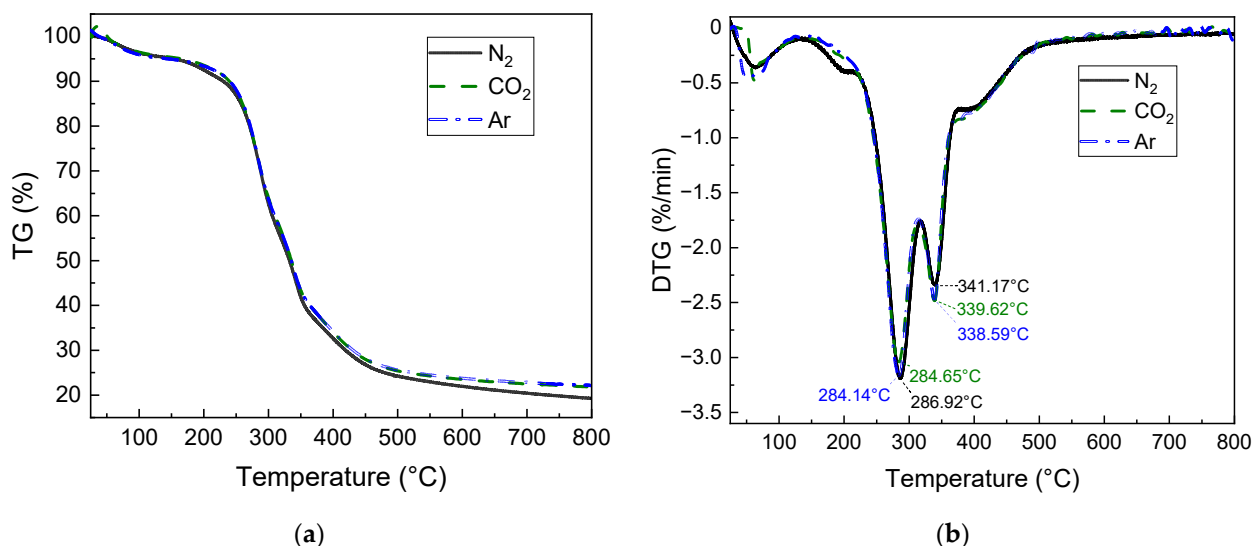


**Figure 2.** TG (a) and DTG (b) curves of BSG pyrolysis under nitrogen, carbon dioxide, and argon atmospheres at a heating rate of 5 K/min.

From the presented figures, it can be noticed that feedstock material is pyrolyzed in the same way under each gas. There were no significant differences in the pyrolysis behavior. The first stage of the process between 25  $^{\circ}C$  and 105  $^{\circ}C$  referred to moisture evaporation. In the temperature range between 250  $^{\circ}C$  and 450  $^{\circ}C$ , BSG lost the highest amount of initial mass, and the mass dropped from around 91.5% to 30% of the initial mass. This zone refers to the main pyrolysis, where volatiles are released from biomass particles. It could be observed that this process was nearly the same for all the considered cases. For every test, there were two peaks where the mass conversion was the highest. The first peak could be observed at a temperature around 284  $^{\circ}C$ , where the mass loss was around 3.2%/min, and the second peak occurred at a temperature close to 340  $^{\circ}C$  with mass loss of around 2.4%/min.

After reaching 450  $^{\circ}C$ , the mass conversion was decelerated, and only residual volatiles were released from the particles. In this range of pyrolysis, it was also assumed that the reactive gas, carbon dioxide, had started to react with char. It was expected that the TG and DTG curves for inert gases would be nearly the same, while for carbon dioxide smaller amount of initial mass would be observed, especially for higher temperatures. From the presented results, the TG curves are closely the same for all gases. It could be

concluded that, in this temperature range, carbon dioxide does not react with the char in a noticeable way. The received curves of BSG pyrolysis are compatible with the literature review [25].

### 3.3. Yield of Products from Intermediate Pyrolysis

The yield of pyrolytic products from the intermediate pyrolysis under an atmosphere of  $N_2$ ,  $CO_2$ , and Ar at 500 °C, 600 °C, and 700 °C is presented in Figure 3. The oil represents the condensable fraction of volatiles and condensed water; the char represents the solid residue remained after the experiment, and the gas refers to light-weight gases which did not condensate in the ice bucket. The yield of products was calculated according to Equations (1)–(3).

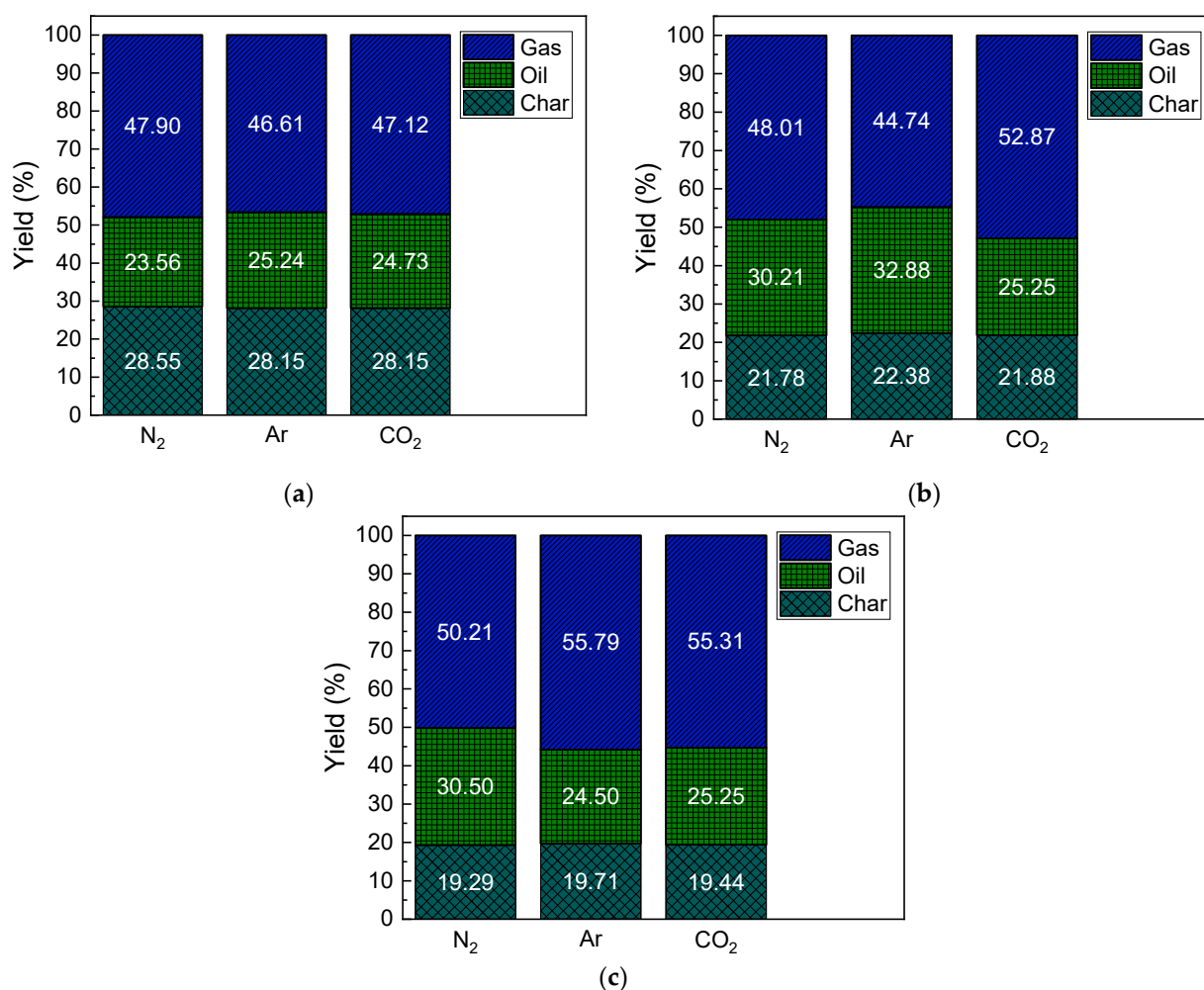


**Figure 3.** Products yields received from pyrolysis of BSG at (a) 500 °C, (b) 600 °C, and (c) 700 °C.

The presented results have confirmed that the carrier gases did not influence the products yields in a noticeable way. In particular, the char content remained at the same level and its yield changed only with temperature from around 28% at 500 °C to 19% at 700 °C. The char content was expected to be lower under the  $CO_2$  atmosphere due to the heterogeneous reaction, and this reaction would be more intensive at higher temperature. In these cases, it could be concluded that the solid fraction did not react with the reactive atmosphere significantly, and the yield of char was nearly the same for  $CO_2$  as for inert gases.

The yield of other products also did not change with the utilization of the carrier gas or even with the temperature. The oil fraction was in the range from 23.56% to 32.88%, and the gas yield was from 44.74% to 55.79% of the initial mass of BSG. A slight disproportion

could be observed at 600 °C where the oil fraction yield was higher for inert gases than for carbon dioxide, and this difference was of around 7.5%.

Obtained results of products yield for intermediate pyrolysis are valid with literature review, and similar results could be found in work [40]. Scientists made an analysis of intermediate pyrolysis of 8 different feedstocks, and char content has been reported from 27–40%, oil yield was from 20% to 47.5%, and gas fraction consisted of 24.5–40.5% of the initial mass of sample. The results of the impact of carrier gas also agree with Reference [28], where difference between yield of char for various gases was around 1.5%.

### 3.4. Analytical Methods of Feedstock and Products Characterization

#### 3.4.1. Ultimate Analysis of Char

The chars from the experiments were collected to analyze their properties, especially the elemental composition. Although the yields of char between various carrier gases were nearly identical, it was worth finding out about the composition of char from different cases. Table 2 presents the results of the ultimate analysis of the chars received under various conditions. Additionally, the atomic ratios of H/C and O/C were included in this table.

**Table 2.** Results of ultimate analysis of BSG char in an air-dry state.

Temperature (°C)	Gas Atmosphere	C (wt%)	H (wt%)	N (wt%)	<sup>a</sup> O (wt%)	H/C	O/C
500	N <sub>2</sub>	65.00	4.25	6.36	24.39	0.785	0.281
	Ar	66.28	4.19	6.59	22.94	0.758	0.260
	CO <sub>2</sub>	67.29	4.15	6.55	22.00	0.740	0.245
600	N <sub>2</sub>	67.02	3.07	6.23	23.68	0.550	0.265
	Ar	67.18	3.14	6.30	23.38	0.561	0.261
	CO <sub>2</sub>	68.60	3.00	6.65	21.75	0.524	0.238
700	N <sub>2</sub>	68.44	2.48	5.94	23.14	0.435	0.254
	Ar	69.08	2.48	5.92	22.52	0.430	0.244
	CO <sub>2</sub>	70.39	2.32	6.22	21.06	0.396	0.224

<sup>a</sup> O: by difference, ash free.

According to the received results, it can be observed that char from pyrolysis under carbon dioxide is slightly richer in carbon. This situation happens at all temperatures considered. The maximal difference in carbon content between chars is around 2%, and the following correlation was observed in every case: CO<sub>2</sub> > Ar > N<sub>2</sub>. Taking into account other elements, it can be observed that the highest nitrogen content is received under CO<sub>2</sub> atmosphere except 500 °C, and this situation has been proven in [41]. Additionally, the smallest amount of oxygen in char is always obtained under a CO<sub>2</sub> atmosphere. From presented results, under CO<sub>2</sub> pyrolysis, chars are characterized by the lowest value of H/C and O/C ratios. The lower the H/C and especially the O/C ratios, the better the quality of the chars, and the char is close to being built with pure carbon, which is the desirable effect in solid fuels [42].

The small differences between the elemental composition can be confirmed according to Reference [43]. Gao et al. used pure nitrogen and a 50/50 mixture of nitrogen and carbon dioxide in lignite pyrolysis at 550, 700, and 800 °C. The differences in carbon content were around 1.2, 3.4, and 1.3%, respectively, at 500, 700, and 800 °C, but in all cases, the carbon chars from nitrogen pyrolysis were richer in carbon. In the work of Luo et al. [44], scientists investigated a pyrolysis of bituminous coal and platanus sawdust under a pure nitrogen and pure carbon dioxide atmosphere. The received results on the elemental composition of the char suggest the small difference in carbon content of 2% and, in this case, the chars obtained under carbon dioxide pyrolysis were also richer in carbon.

#### 3.4.2. Combustion Characteristics of Selected Chars

From the results of the ultimate analysis, chars that were characterized by the lowest and highest carbon content at the lowest and highest investigated temperature were consid-

ered for further analysis. For this reason, the chars obtained from pyrolysis under nitrogen and carbon dioxide atmosphere at 500 and 700 °C were selected. The chars were analyzed by the thermogravimetric analysis and were combusted under air conditions. The results of char combustion behavior are presented in Figure 4. Based on these results, the ignition and burnout temperatures were determined, and results are presented in Table 3.

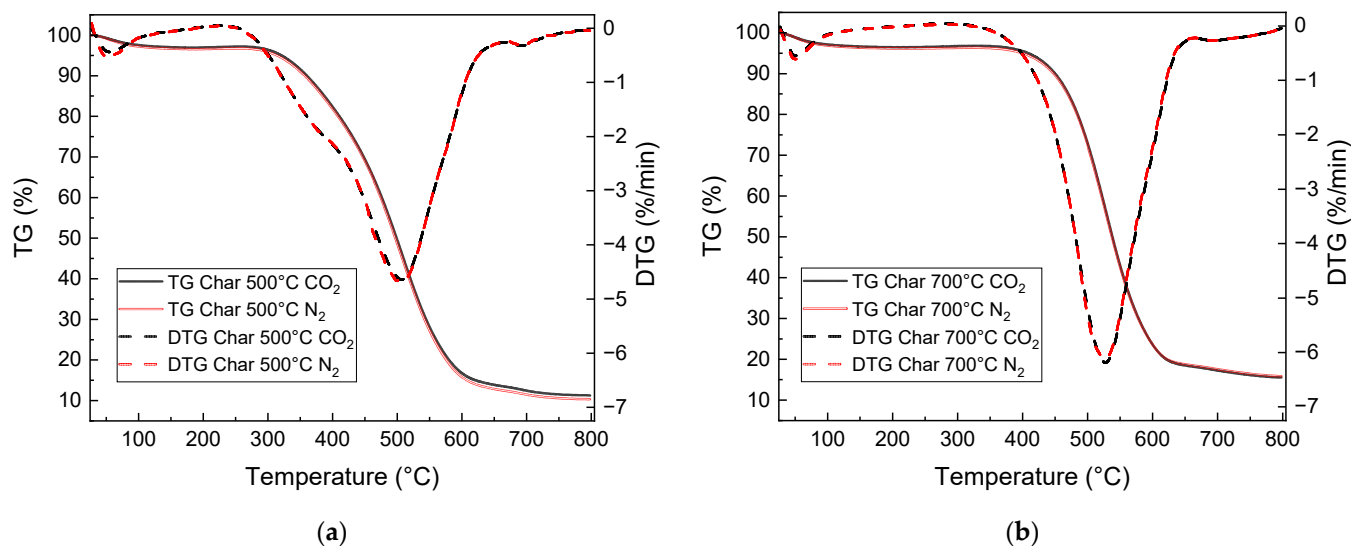


**Figure 4.** TG and DTG curves of char combustion which was obtained from pyrolysis under carbon dioxide and nitrogen atmosphere at (a) 500 °C and (b) 700 °C.

**Table 3.** Ignition and burnout temperatures for chars obtained at 500 and 700 °C under carbon dioxide and nitrogen atmosphere.

Sample Name	Ignition Temperature (°C)	Burnout Temperature (°C)
Char_500_CO <sub>2</sub>	400.1	711.9
Char_500_N <sub>2</sub>	397.0	710.8
Char_700_CO <sub>2</sub>	466.3	739.5
Char_700_N <sub>2</sub>	463.4	739.6

The small differences in the carbon content in the chars did not reflect the combustion behavior of the chars considered. The curves overlap by themselves, and for this reason, it could be concluded that the gaseous atmosphere of pyrolysis did not influence the combustion behavior of received chars. The conclusion can be confirmed by the similar ignition and burnout temperatures of chars. Only the temperature of pyrolysis had an impact on the values of the ignition and burnout temperatures. The ignition temperature of the chars was around 66 K higher for the char obtained at 700 °C. The same correlation was observed for the burnout temperature, but the difference was around 29 °C.

### 3.5. Characteristics of Organic Fraction of Oil

The oils collected from the experiments consisted of two separate phases: the aqueous phase (water + soluble compounds) and the organic phase. The phases had been separated, and for further analysis, only the organic fraction was involved. Gas chromatography was performed, where organic compounds were determined. The obtained results allowed the classification of the compounds on the basis of their functional group. The solutions of this classification are presented in Figure 5. Additionally, in Table 4 is the list of detected compounds and their relative content in the organic fraction of oil.

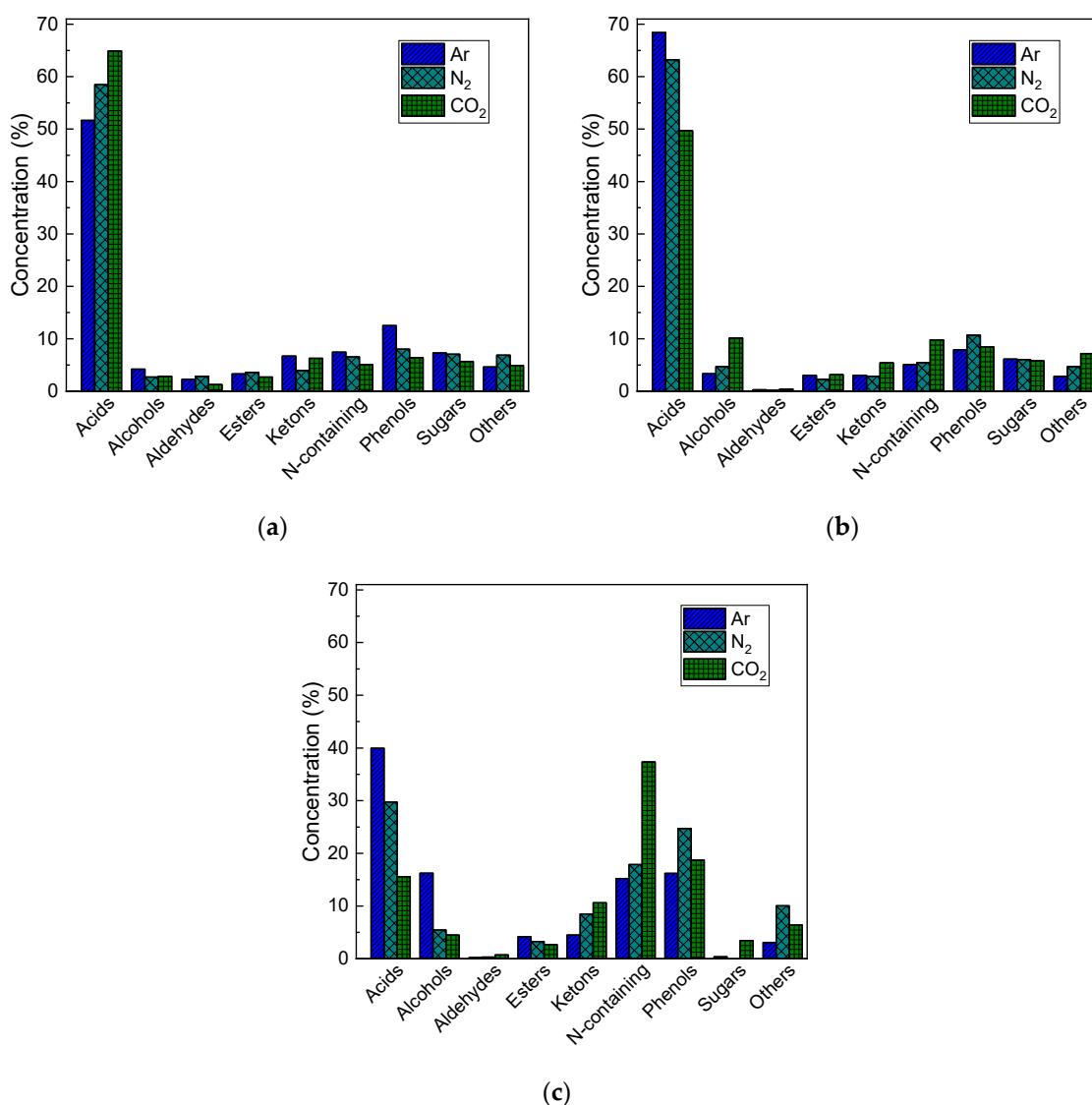


**Figure 5.** Relative content of different groups of chemicals in organic fraction of oil received under argon, nitrogen, and carbon dioxide at (a) 500 °C, (b) 600 °C, and (c) 700 °C.

Despite the similar yields of the oil under respected gases, from Figure 5 and Table 4, it could be observed that a diversified structure of oil and a content of selected compound are different for every gas. The main group of compounds were acids, which was confirmed in work [25], and this group of compounds was dominant at every pyrolysis temperature and used carrier gas. At 600 °C and 700 °C, it was observed that under an argon atmosphere, the higher amount of acids evolved while the lowest amount was under carbon dioxide. The reverse situation occurred for pyrolysis at 500 °C, where at this temperature, carbon dioxide promoted the higher content of acids. A high amount of acids in the oil could be result of significant content of lipids up to even 13% in the BSG structure [45]. Among the acid compounds, the n-Hexadecanoic acid was dominant, and its concentration was dependent on the carrier used in the following line: Ar > N<sub>2</sub> > CO<sub>2</sub> at all temperatures. Another major compound among acidic group was 9,12-Octadecadienoic acid (Z,Z)-, and the highest content of 25.17% was determined at 500 °C under CO<sub>2</sub> atmosphere. For 600 °C and 700 °C, the same correlation was recorded as for the previous compound, but at 700 °C under CO<sub>2</sub>, the compound was not detected. The last major compound identified was oleic acid, and its concentration was the highest for nitrogen atmosphere at 500 °C and 600 °C.

Another large group of compounds include nitrogen in their structure. The presence of these compounds in oil would be the result of the destruction of proteins that also have

significant content in BSG up to 31% [46,47]. The N-containing compounds had the highest share in the oil structure at 700 °C and under CO<sub>2</sub>, and their relative content was around 40%. For nitrogen and argon, N-containing compounds consisted around 18 and 15%, respectively, at the same temperature. The lower the temperature, the significant lower the number of N-containing compounds in the oil structure, and the relative content became the same for each gas. In this group, the main determined compound was 3-Octanamine received under carbon dioxide at 700 °C with a relative content of around 11.3%.

As the temperature of pyrolysis increased, the total phenol content grew, and the highest concentration was observed at 700 °C under a nitrogen atmosphere. In this atmosphere, the phenol content increased from around 8% at 500 °C to 30% at 700 °C. The dominant compound in this group was p-cresol, which was observed under all atmospheres at all temperatures. The highest concentration of p-cresol was determined under nitrogen at 700 °C. The presence of p-cresol could be the result of thermal degradation of lignin structures [48].

Analyzing Table 4 and Figure 5, it is worth also mentioning the content of derivatives of saccharides, and with it the oil, galacto-heptulose, that was determined. Its concentration is noticeable at 500 and 600 °C for all gases, and it was around 6–7%. At 700 °C, the compound was measured only in the case of carbon dioxide and was 3.45% of relative content. The presence of galcato-heptulose could be the result of saccharide degradation [49].

Presented analysis confirms that acids have the major share in oil structure with relative content of 52–65%, 49–68%, and 26–40%, respectively, at 500, 600, and 700 °C. The content of acids was dependent on used carrier gas. At higher temperatures, argon promoted higher concentration of acids where the lowest was observed for carbon dioxide. The diversified structure of oil received under various atmospheres at the same temperature was also confirmed in works [28,29,50].

**Table 4.** Chemical compositions of the oils obtained under argon, nitrogen, and carbon dioxide.

Compound	Formula	Relative Content at Different Conditions (%)								
		500 °C			600 °C			700 °C		
		Ar	N <sub>2</sub>	CO <sub>2</sub>	Ar	N <sub>2</sub>	CO <sub>2</sub>	Ar	N <sub>2</sub>	CO <sub>2</sub>
Acids										
Propanoic acid	C <sub>3</sub> H <sub>6</sub> O <sub>2</sub>	0.98	1.17	0.74	1.29	0.96	1.53	0.00	2.36	1.33
Propanoic acid, 2-methyl-	C <sub>4</sub> H <sub>8</sub> O <sub>2</sub>	0.00	0.18	0.11	0.00	0.00	0.00	0.00	0.68	0.00
Butanoic acid, 3-methyl-	C <sub>5</sub> H <sub>10</sub> O <sub>2</sub>	0.43	0.33	0.00	0.00	0.95	0.00	0.00	0.33	0.00
Undec-10-ynoic acid	C <sub>11</sub> H <sub>18</sub> O <sub>2</sub>	0.00	0.00	0.00	0.47	0.33	0.52	0.55	0.32	0.67
n-Hexadecanoic acid	C <sub>16</sub> H <sub>32</sub> O <sub>2</sub>	32.46	27.94	29.36	34.76	32.72	22.96	32.72	22.74	12.83
Oleic Acid	C <sub>18</sub> H <sub>34</sub> O <sub>2</sub>	7.78	10.36	9.51	9.68	10.15	8.97	2.93	1.72	0.76
9,12-Octadecadienoic acid (Z,Z)-	C <sub>18</sub> H <sub>32</sub> O <sub>2</sub>	10.02	18.49	25.17	22.21	18.10	15.71	3.76	1.59	0.00
Alcohols										
2-Pentanone, 4-hydroxy-4-methyl-	C <sub>6</sub> H <sub>12</sub> O <sub>2</sub>	0.70	0.59	0.83	1.20	0.47	0.88	14.33	2.71	3.02
2-Furanmethanol	C <sub>5</sub> H <sub>6</sub> O <sub>2</sub>	0.98	0.75	0.60	0.97	0.72	1.84	0.18	2.13	0.00
5,7-Octadien-3-ol, 2,4,4,7-tetramethyl-, (E)-	C <sub>12</sub> H <sub>22</sub> O	0.19	0.23	0.19	0.00	0.00	0.00	0.00	0.31	0.00
1-Heptatriacotanol	C <sub>37</sub> H <sub>76</sub> O	2.34	1.12	1.22	1.17	3.50	7.42	0.66	0.00	0.93
3-Cyclohexen-1-ol, 1-methyl-	C <sub>10</sub> H <sub>18</sub> O	1.01	0.74	0.75	0.36	0.49	2.26	0.00	2.34	1.94
4,7-Methano-1H-inden-1-ol, 3a,4,7,7a-tetrahydro-	C <sub>10</sub> H <sub>12</sub> O	0.00	0.12	0.10	0.17	0.19	0.09	1.38	1.23	0.87
Bicyclo [2.2.1]heptan-2-ol, 7,7-dimethyl-, acetate	C <sub>11</sub> H <sub>18</sub> O <sub>2</sub>	0.86	0.26	0.11	1.01	0.33	0.94	2.61	2.34	1.51
Tetracyclo [4.4.1.1(7,10).0(2,5)]dodec-3-en-11-ol	C <sub>12</sub> H <sub>16</sub> O	0.00	0.00	0.00	0.00	0.00	0.00	1.05	0.32	0.55
Aldehydes										

Table 4. Cont.

Compound	Formula	Relative Content at Different Conditions (%)								
		500 °C			600 °C			700 °C		
		Ar	N <sub>2</sub>	CO <sub>2</sub>	Ar	N <sub>2</sub>	CO <sub>2</sub>	Ar	N <sub>2</sub>	CO <sub>2</sub>
2,3,4,5,6,7,8-Heptahydroxyoctanal	C <sub>8</sub> H <sub>16</sub> O <sub>8</sub>	1.33	1.33	1.11	0.00	0.00	0.00	0.00	0.22	0.00
Esters										
2-Propanone, 1-(acetyloxy)-	C <sub>5</sub> H <sub>8</sub> O <sub>3</sub>	1.74	1.68	1.63	0.61	0.66	1.16	0.20	0.28	0.00
2,5-Octadecadiynoic acid, methyl ester	C <sub>19</sub> H <sub>34</sub> O <sub>2</sub>	0.00	0.52	0.21	0.64	0.32	0.90	0.83	0.36	1.27
2-Octen-1-ol, 3,7-dimethyl-, isobutyrate, (Z)-	C <sub>14</sub> H <sub>26</sub> O <sub>2</sub>	0.40	0.30	0.18	0.94	0.50	0.57	0.98	0.50	0.00
Propanoic acid, ethenyl ester	C <sub>5</sub> H <sub>10</sub> O <sub>2</sub>	0.21	0.37	0.15	0.00	0.00	0.00	0.00	0.22	0.00
2-Acetoxy-1,2-dihydronaphthalene	C <sub>12</sub> H <sub>12</sub> O <sub>2</sub>	0.95	0.71	0.54	0.81	0.78	0.52	2.17	1.90	1.41
Eters										
Geranyl vinyl ether	C <sub>12</sub> H <sub>20</sub> O	0.88	0.78	1.25	0.54	0.24	2.46	0.64	1.57	0.94
Ketons										
3-Hexen-2-one	C <sub>6</sub> H <sub>10</sub> O	0.17	0.00	0.27	0.00	0.00	0.25	0.27	1.01	3.97
2-Butanone, 4-cyclohexyl-	C <sub>10</sub> H <sub>18</sub> O	0.18	0.26	0.19	0.00	0.00	0.00	0.00	0.48	0.00
Cyclohexanone, 2-methyl-	C <sub>10</sub> H <sub>18</sub> O	1.46	1.26	1.51	1.04	1.38	0.96	0.00	0.96	0.94
2H-Pyran-2-one, tetrahydro-4-(2-methyl-3-methylene-1-buten-4-yl)-	C <sub>11</sub> H <sub>16</sub> O <sub>2</sub>	0.33	0.28	0.64	0.46	0.47	0.91	0.25	0.16	1.40
3H-Cyclodeca[b]furan-2-one, 4,9-dihydroxy-6-methyl-3,10-dimethylene-3a,4,7,8,9,10,11,11a-octahydro-	C <sub>15</sub> H <sub>20</sub> O <sub>4</sub>	0.91	1.48	0.16	0.28	0.19	0.40	0.22	0.12	0.72
Cyclohexanone, 2-(2-butyryl)-	C <sub>10</sub> H <sub>14</sub> O	0.93	0.00	1.72	0.00	0.00	0.00	0.00	0.00	0.00
N-Containing										
2-Propen-1-amine, N,N-bis(1-methylethyl)-	C <sub>4</sub> H <sub>9</sub> NO	0.63	0.32	0.40	0.26	0.32	0.76	0.57	1.56	2.29
2-Pyrroline, 1,2-dimethyl-	C <sub>11</sub> H <sub>18</sub> N <sub>2</sub> O <sub>2</sub>	0.66	0.25	0.48	0.45	0.95	0.72	0.58	1.55	1.56
3-Octanamine	C <sub>10</sub> H <sub>19</sub> N	0.00	0.00	0.14	0.00	0.00	0.00	0.00	0.00	11.29
3-Pyrrolidinol	C <sub>4</sub> H <sub>9</sub> NO	0.47	0.17	0.14	0.00	0.00	1.54	0.00	0.00	0.00
4-(2,5-Dihydro-3-methoxyphenyl)butylamine	C <sub>18</sub> H <sub>35</sub> NO	0.00	0.13	0.00	0.37	0.38	0.42	0.72	0.26	0.70
4-(2,5-Dihydro-3-methoxyphenyl)butylamine	C <sub>8</sub> H <sub>19</sub> N	0.53	1.02	0.59	0.65	1.14	0.71	0.00	0.86	0.63
4-Piperidinone, 2,2,6,6-tetramethyl-	C <sub>9</sub> H <sub>19</sub> N	0.18	0.00	0.10	0.00	0.00	0.45	1.15	1.80	8.38
7-Azabicyclo [4.1.0]heptane, 1-methyl-4-(1-methylethyl)-	C <sub>11</sub> H <sub>19</sub> NO	0.50	0.00	0.00	0.16	0.00	0.24	0.00	0.86	0.54
9-Octadecenamide, (Z)-	C <sub>11</sub> H <sub>19</sub> NO	0.32	0.82	0.00	0.52	0.88	0.82	9.93	0.00	1.73
Acetamide, N-methyl-N-[4-(3-hydroxypyrrolidinyl)-2-butyryl]-	C <sub>10</sub> H <sub>13</sub> N <sub>3</sub>	0.91	1.01	0.00	0.00	0.00	0.53	0.26	5.23	1.27
Debrisoquine	C <sub>9</sub> H <sub>17</sub> NO	0.32	0.00	0.11	0.00	0.00	0.00	0.00	1.14	0.00
Ethanimidic acid, ethyl ester	C <sub>5</sub> H <sub>5</sub> N	0.55	1.06	0.78	0.00	0.00	0.00	0.00	0.66	0.00
Hydrazinecarboxylic acid, phenylmethyl ester	C <sub>6</sub> H <sub>13</sub> N	0.15	0.16	0.19	0.36	0.22	0.35	0.59	1.08	0.61
N-[3-[N-Aziridyl]propylidene]-1-azacycloheptylamine	C <sub>6</sub> H <sub>11</sub> N	0.00	0.00	0.00	0.23	0.23	0.22	0.30	0.68	3.67
Piperidine, 1-methyl-	C <sub>10</sub> H <sub>21</sub> N <sub>3</sub>	1.00	0.42	1.13	0.94	0.51	1.12	0.00	0.00	0.00
Pyridine	C <sub>8</sub> H <sub>10</sub> N <sub>2</sub> O <sub>2</sub>	0.91	0.91	0.70	0.59	0.79	1.01	0.37	0.00	2.37
Pyridine, 2-methyl-	C <sub>6</sub> H <sub>7</sub> N	0.32	0.28	0.30	0.56	0.00	0.88	0.74	2.21	2.29

Table 4. Cont.

Compound	Formula	Relative Content at Different Conditions (%)								
		500 °C			600 °C			700 °C		
		Ar	N <sub>2</sub>	CO <sub>2</sub>	Ar	N <sub>2</sub>	CO <sub>2</sub>	Ar	N <sub>2</sub>	CO <sub>2</sub>
Phenols										
Phenol	C <sub>6</sub> H <sub>6</sub> O	0.98	1.09	0.74	0.38	2.63	2.00	0.57	6.45	4.47
o-Cresol	C <sub>7</sub> H <sub>8</sub> O	0.16	0.19	0.14	0.54	0.64	0.39	1.00	1.87	1.32
p-Cresol	C <sub>7</sub> H <sub>8</sub> O	3.95	3.04	2.32	6.23	6.77	5.65	10.26	14.87	9.97
o-Ethylphenol	C <sub>8</sub> H <sub>10</sub> O	1.08	1.27	1.16	1.50	3.05	1.81	0.44	3.82	2.93
Mequinol	C <sub>7</sub> H <sub>8</sub> O <sub>2</sub>	1.35	1.32	1.04	0.53	0.64	0.43	1.78	1.02	0.63
4-Ethyl-2-methoxyphenol	C <sub>9</sub> H <sub>12</sub> O <sub>2</sub>	1.25	1.24	1.15	0.00	0.00	0.00	0.00	0.00	0.00
Phenol, 2,6-dimethoxy-	C <sub>8</sub> H <sub>10</sub> O <sub>3</sub>	0.64	0.71	0.55	0.00	0.00	0.00	0.00	0.20	0.00
Phenol, 4-methoxy-3-(methoxymethyl)-	C <sub>9</sub> H <sub>12</sub> O <sub>3</sub>	0.41	0.43	0.45	0.00	0.00	0.00	0.00	0.32	0.00
Androst-5,7-dien-3-ol-17-one	C <sub>19</sub> H <sub>26</sub> O <sub>2</sub>	3.78	0.00	0.00	0.22	0.00	0.00	2.59	0.00	2.31
Sugars										
Galacto-heptulose	C <sub>7</sub> H <sub>14</sub> O <sub>7</sub>	7.29	7.06	5.67	6.13	6.02	5.79	0.39	0.00	3.45
Other										
Cyclopropane, 2-(1,1-dimethyl-2-pentenyl)-1,1-dimethyl- R-Limonene	C <sub>12</sub> H <sub>22</sub>	0.36	0.36	0.30	0.00	0.00	0.00	0.00	0.60	0.00
Indene	C <sub>9</sub> H <sub>8</sub>	1.44	0.75	0.47	0.00	0.00	0.00	0.00	0.62	0.00
1,5,5-Trimethyl-6-methylene-cyclohexene	C <sub>10</sub> H <sub>16</sub>	0.34	0.37	0.31	0.16	0.49	0.50	0.44	1.08	0.87
		0.00	0.36	0.38	0.36	0.61	0.34	1.40	0.00	0.65

#### 4. Conclusions

In this work, intermediate pyrolysis of the brewer's spent grains was carried out in a horizontal fixed bed reactor at three temperatures of 500, 600, and 700 °C. The study focused on the analysis of the influence of carrier gas on the pyrolytic products received under the following conditions: argon, carbon dioxide, and nitrogen. The conducted analysis allows to draw the following conclusions:

1. According to thermogravimetric analysis, there were no significant differences in the pyrolysis behavior of brewer's spent grain under argon, nitrogen, and carbon dioxide with a heating rate of 5 K/min. The maximum conversion of samples was almost the same for each gas at 284 °C.
2. Intermediate pyrolysis of BSG delivered pyrolytic products independently of the carrier gas. Only temperature had an impact on product concentrations. Especially the char content dropped from around 28.5% to 19.5% as the temperature increased.
3. The ultimate analysis showed that the char received under carbon dioxide was richer in carbon by approximately 2% at all temperatures.
4. The selected chars received under various carrier gases had the same combustion properties as the ignition and burnout temperatures.
5. Analyzing oil composition, the most dominant group of organic compounds was acids with a maximum content of 68% at 600 °C under an argon atmosphere. The presented analysis showed the correlation between the content of acids and the carrier gas as follows: Ar > N<sub>2</sub> > CO<sub>2</sub>. at 600 °C and 700 °C, less acids could be obtained in the case of carbon dioxide relative to inert gases.
6. The highest content in the oil was n-Hexadecanoic acid, and it could be a result of degradation of fats. Carbon dioxide promotes a lower concentration of this compound in the oil at 600 °C and 700 °C.
7. The inert atmosphere did not influence the yield of N-containing compounds in oil. at 600 °C and 700 °C, argon provided a higher amount of these compounds.
8. According to the results, it is worth considering the carbon dioxide as the carrier gas in the char production via intermediate pyrolysis. Char obtained under CO<sub>2</sub> is

characterized by the highest carbon content. Additionally, carbon dioxide is used, which indirectly may lead to decrease of CO<sub>2</sub> in the environment.

**Author Contributions:** Conceptualization, A.B., A.M. and W.J.; methodology, A.B., A.M. and W.J.; software, A.B.; validation, A.B., M.S. and A.M.; formal analysis, A.M. and W.J.; investigation, A.B. and M.S.; resources, A.B., A.M. and W.J.; data curation, A.B., K.S. and Ł.M.; writing—original draft preparation, A.B., K.S. and Ł.M.; writing—review and editing, A.M., W.J. and M.S.; visualization, A.B., K.S. and Ł.M.; supervision, A.M. and W.J.; project administration, A.M.; funding acquisition, A.M. All authors have read and agreed to the published version of the manuscript.

**Funding:** This work was supported by the Ministry of Science and Higher Education, Poland [grant AGH UST no. 16.16.110.663].

**Institutional Review Board Statement:** Not applicable.

**Informed Consent Statement:** Not applicable.

**Data Availability Statement:** Not applicable.

**Conflicts of Interest:** The authors declare no conflict of interest.

## References

1. Directive 2009/30/EC Directive 2009/30/EC of the European Parliament and of the Council of 23 April 2009 Amending Directive 98/70/EC as Regards the Specification of Petrol, Diesel and Gas-Oil and Introducing a Mechanism to Monitor and Reduce Greenhouse Gas Emissions and Amend. 2009. Available online: <https://eur-lex.europa.eu/legal-content/EN/TXT/?uri=celex%3A32009L0030> (accessed on 1 October 2021).
2. Nathan, A.J.; Scobell, A. Summary for Policymakers. *Foreign Aff.* **2014**, *91*, 1–30. [CrossRef]
3. Mohr, S.H.; Wang, J.; Ellem, G.; Ward, J.; Giurco, D. Projection of world fossil fuels by country. *Fuel* **2015**, *141*, 120–135. [CrossRef]
4. Poskart, A.; Skrzyński, M.; Sajdak, M.; Zajemska, M.; Skibiński, A. Management of Lignocellulosic Waste towards Energy Recovery by Pyrolysis in the Framework of Circular Economy Strategy. *Energies* **2021**, *14*, 5864. [CrossRef]
5. Anisimova, N. The capability to reduce primary energy demand in EU housing. *Energy Build.* **2011**, *43*, 2747–2751. [CrossRef]
6. Global Bioenergy Statistics. 2019. Available online: [http://www.worldbioenergy.org/uploads/-191129%20WBA%20GBS%202019\\_HQ.pdf](http://www.worldbioenergy.org/uploads/-191129%20WBA%20GBS%202019_HQ.pdf) (accessed on 1 October 2021).
7. European Union. Directive 2009/28/EC Directive 2009/28/EC of the European Parliament and of the Council of 23 April 2009 on the promotion of the use of energy from renewable sources and amending and subsequently repealing Directives 2001/77/EC and 2003/30/EC. *Off. J. Eur. Union* **2009**, *5*, 2009.
8. Motghare, K.A.; Rathod, A.P.; Wasewar, K.L.; Labhsetwar, N.K. Comparative study of different waste biomass for energy application. *Waste Manag.* **2016**, *47*, 40–45. [CrossRef] [PubMed]
9. García, R.; Pizarro, C.; Álvarez, A.; Lavín, A.G.; Bueno, J.L. Study of biomass combustion wastes. *Fuel* **2015**, *148*, 152–159. [CrossRef]
10. Gunasee, S.D.; Carrier, M.; Gorgens, J.F.; Mohee, R. Pyrolysis and combustion of municipal solid wastes: Evaluation of synergistic effects using TGA-MS. *J. Anal. Appl. Pyrolysis* **2016**, *121*, 50–61. [CrossRef]
11. Wang, X.; Zhang, J.; Bai, S.; Zhang, L.; Li, Y.; Mikulčić, H.; Chen, J.; Wang, L.; Tan, H. Effect of pyrolysis upgrading temperature on particulate matter emissions from lignite semi-char combustion. *Energy Convers. Manag.* **2019**, *195*, 384–391. [CrossRef]
12. Kaczor, Z.; Buliński, Z.; Werle, S. Modelling approaches to waste biomass pyrolysis: A review. *Renew. Energy* **2020**, *159*, 427–443. [CrossRef]
13. Mlonka-Mędrala, A.; Evangelopoulos, P.; Sieradzka, M.; Zajemska, M.; Magdziarz, A. Pyrolysis of agricultural waste biomass towards production of gas fuel and high-quality char: Experimental and numerical investigations. *Fuel* **2021**, *296*, 120611. [CrossRef]
14. Glushkov, D.; Nyashina, G.; Shvets, A.; Pereira, A.; Ramanathan, A. Current Status of the Pyrolysis and Gasification Mechanism of Biomass. *Energies* **2021**, *14*, 7541. [CrossRef]
15. Eurostat. Happy International Beer Day! Products Eurostat News. Available online: <https://ec.europa.eu/eurostat/web/products-eurostat-news/-/edn-20210805-1> (accessed on 1 October 2021).
16. Agro Industry Młoto Browarnicze–Stary Problem, Nowe Pomysły-Agroindustry.pl. Available online: <https://www.agroindustry.pl/index.php/2021/01/12/mloto-browarnicze-stary-problem-nowe-pomysly/> (accessed on 28 May 2021).
17. Rachwał, K.; Waśko, A.; Gustaw, K.; Polak-Berecka, M. Utilization of brewery wastes in food industry. *PeerJ* **2020**, *8*, e9427. [CrossRef] [PubMed]
18. Mussatto, S.I.; Dragone, G.; Roberto, I.C. Brewers' spent grain: Generation, characteristics and potential applications. *J. Cereal Sci.* **2006**, *43*, 1–14. [CrossRef]
19. Mutlu, Ö.Ç.; Büchner, D.; Theurich, S.; Zeng, T. Combined Use of Solar and Biomass Energy for Sustainable and Cost-Effective Low-Temperature Drying of Food Processing Residues on Industrial-Scale. *Energies* **2021**, *14*, 561. [CrossRef]

20. Celaya, A.M.; Lade, A.T.; Goldfarb, J.L. Co-combustion of brewer's spent grains and Illinois No. 6 coal: Impact of blend ratio on pyrolysis and oxidation behavior. *Fuel Process. Technol.* **2015**, *129*, 39–51. [[CrossRef](#)]
21. Arranz, J.I.; Sepúlveda, F.J.; Montero, I.; Romero, P.; Miranda, M.T. Feasibility Analysis of Brewers' Spent Grain for Energy Use: Waste and Experimental Pellets. *Appl. Sci.* **2021**, *11*, 2740. [[CrossRef](#)]
22. Gil-Castell, O.; Mascia, N.; Primaz, C.; Vásquez-Garay, F.; Baschetti, M.G.; Ribes-Greus, A. Brewer's spent grains as biofuels in combustion-based energy recovery processes: Evaluation of thermo-oxidative decomposition. *Fuel* **2022**, *312*, 122955. [[CrossRef](#)]
23. Čater, M.; Fanel, L.; Malovrh, Š.; Marinšek Logar, R. Biogas production from brewery spent grain enhanced by bioaugmentation with hydrolytic anaerobic bacteria. *Bioresour. Technol.* **2015**, *186*, 261–269. [[CrossRef](#)]
24. Yin, X.; Jishi, Z.; Yi, M. Preparation and Application of Biochar from Brewery's Spent Grain and Sewage Sludge. *Open Chem. Eng. J.* **2015**, *9*, 14–19. [[CrossRef](#)]
25. Mahmood, A.S.N.; Brammer, J.G.; Hornung, A.; Steele, A.; Poulston, S. The intermediate pyrolysis and catalytic steam reforming of Brewers spent grain. *J. Anal. Appl. Pyrolysis* **2013**, *103*, 328–342. [[CrossRef](#)]
26. Borel, L.D.M.S.; Lira, T.S.; Ribeiro, J.A.; Ataíde, C.H.; Barrozo, M.A.S. Pyrolysis of brewer's spent grain: Kinetic study and products identification. *Ind. Crops Prod.* **2018**, *121*, 388–395. [[CrossRef](#)]
27. Olszewski, M.P.; Arauzo, P.J.; Maziarka, P.A.; Ronsse, F.; Kruse, A. Pyrolysis Kinetics of Hydrochars Produced from Brewer's Spent Grains. *Catalysts* **2019**, *9*, 625. [[CrossRef](#)]
28. Zhang, H.; Xiao, R.; Wang, D.; He, G.; Shao, S.; Zhang, J.; Zhong, Z. Biomass fast pyrolysis in a fluidized bed reactor under N<sub>2</sub>, CO<sub>2</sub>, CO, CH<sub>4</sub> and H<sub>2</sub> atmospheres. *Bioresour. Technol.* **2011**, *102*, 4258–4264. [[CrossRef](#)]
29. Liu, J.; Li, G.Q.; Chen, L.; Wang, Y.; Xu, Y.; Qiao, X.X.; Zhang, Y.F. Effects of atmospheric gas on pyrolysis characteristics of briquetted lignite and surface properties of semi-char. *Fuel Process. Technol.* **2016**, *151*, 40–49. [[CrossRef](#)]
30. Zhang, B.; Zhang, J. Influence of Reaction Atmosphere (N<sub>2</sub>, CO, CO<sub>2</sub>, and H<sub>2</sub>) on ZSM-5 Catalyzed Microwave-Induced Fast Pyrolysis of Medicinal Herb Residue for Biofuel Production. *Energy Fuels* **2017**, *31*, 9627–9632. [[CrossRef](#)]
31. Mellin, P.; Yu, X.; Yang, W.; Blasiak, W. Influence of Reaction Atmosphere (H<sub>2</sub>O, N<sub>2</sub>, H<sub>2</sub>, CO<sub>2</sub>, CO) on Fluidized-Bed Fast Pyrolysis of Biomass Using Detailed Tar Vapor Chemistry in Computational Fluid Dynamics. *Ind. Eng. Chem. Res.* **2015**, *54*, 8344–8355. [[CrossRef](#)]
32. Yang, Q.; Zhou, H.; Bartocci, P.; Fantozzi, F.; Mašek, O.; Agblevor, F.A.; Wei, Z.; Yang, H.; Chen, H.; Lu, X.; et al. Prospective contributions of biomass pyrolysis to China's 2050 carbon reduction and renewable energy goals. *Nat. Commun.* **2021**, *12*, 1698. [[CrossRef](#)] [[PubMed](#)]
33. Speight, J.G. Upgrading by Gasification. In *Heavy Oil Recovery and Upgrading*; Gulf Professional Publishing: Houston, TX, USA, 2019; pp. 559–614. [[CrossRef](#)]
34. Jerzak, W.; Bieniek, A.; Magdziarz, A. Multifaceted analysis of products from the intermediate co-pyrolysis of biomass with Tetra Pak waste. *Int. J. Hydrogen Energy* **2021**. [[CrossRef](#)]
35. Soest, P.J. Van Use of Detergents in the Analysis of Fibrous Feeds. II. A Rapid Method for the Determination of Fiber and Lignin. *J. Assoc. Off. Anal. Chem.* **1990**, *73*, 491–497. [[CrossRef](#)]
36. Li, Q.; Zhao, C.; Chen, X.; Wu, W.; Li, Y. Comparison of pulverized coal combustion in air and in O<sub>2</sub>/CO<sub>2</sub> mixtures by thermo-gravimetric analysis. *J. Anal. Appl. Pyrolysis* **2009**, *85*, 521–528. [[CrossRef](#)]
37. Ding, T.; Li, S.; Xie, J.; Song, W.; Yao, J.; Lin, W. Rapid Pyrolysis of Wheat Straw in a Bench-Scale Circulating Fluidized-Bed Downer Reactor. *Chem. Eng. Technol.* **2012**, *35*, 2170–2176. [[CrossRef](#)]
38. Basu, P. *Biomass Gasification, Pyrolysis and Torrefaction: Practical Design and Theory*; Elsevier Inc.: Amsterdam, The Netherlands, 2013; ISBN 9780123964885.
39. Olszewski, M.P.; Arauzo, P.J.; Wądrzyk, M.; Kruse, A. Py-GC-MS of hydrochars produced from brewer's spent grains. *J. Anal. Appl. Pyrolysis* **2019**, *140*, 255–263. [[CrossRef](#)]
40. Tinwala, F.; Mohanty, P.; Parmar, S.; Patel, A.; Pant, K.K. Intermediate pyrolysis of agro-industrial biomasses in bench-scale pyrolyser: Product yields and its characterization. *Bioresour. Technol.* **2015**, *188*, 258–264. [[CrossRef](#)] [[PubMed](#)]
41. Aljaziri, J.; Gautam, R.; Alturkistani, S.; Fiene, G.M.; Tester, M.; Sarathy, S.M. On the effects of CO<sub>2</sub> atmosphere in the pyrolysis of *Salicornia bigelovii*. *Bioresour. Technol. Rep.* **2022**, *17*, 100950. [[CrossRef](#)]
42. Smoot, L.D. General Characteristics of Coal. In *Pulverized-Coal Combustion and Gasification*; Springer: Boston, MA, USA, 1979; pp. 123–132. [[CrossRef](#)]
43. Gao, S.P.; Zhao, J.T.; Wang, Z.Q.; Wang, J.F.; Fang, Y.T.; Huang, J.J. Effect of CO<sub>2</sub> on pyrolysis behaviors of lignite. *Ranliao Huaxue Xuebao/J. Fuel Chem. Technol.* **2013**, *41*, 257–264. [[CrossRef](#)]
44. Luo, Y.; Ben, H.; Wu, Z.; Nie, K.; Han, G.; Jiang, W. Impact of CO<sub>2</sub> on Pyrolysis Products of Bituminous Coal and Platanus Sawdust. *Polymers* **2019**, *11*, 1370. [[CrossRef](#)] [[PubMed](#)]
45. Lynch, K.M.; Steffen, E.J.; Arendt, E.K. Brewers' spent grain: A review with an emphasis on food and health. *J. Inst. Brew.* **2016**, *122*, 553–568. [[CrossRef](#)]
46. Ikram, S.; Huang, L.Y.; Zhang, H.; Wang, J.; Yin, M. Composition and Nutrient Value Proposition of Brewers Spent Grain. *J. Food Sci.* **2017**, *82*, 2232–2242. [[CrossRef](#)]

47. Santos, M.; Jiménez, J.J.; Bartolomé, B.; Gómez-Cordovés, C.; Del Nozal, M.J. Variability of brewer's spent grain within a brewery. *Food Chem.* **2003**, *80*, 17–21. [[CrossRef](#)]
48. Nonaka, H.; Yamamoto, R.; Funaoka, M. Selective conversion of hardwood lignin into syringyl methyl benzofuran using p-cresol. *Polym. J.* **2016**, *48*, 977–981. [[CrossRef](#)]
49. Moldoveanu, S.C. Chapter 16 Pyrolysis of Carbohydrates. *Tech. Instrum. Anal. Chem.* **2010**, *28*, 419–470. [[CrossRef](#)]
50. Tarves, P.C.; Mullen, C.A.; Boateng, A.A. Effects of Various Reactive Gas Atmospheres on the Properties of Bio-Oils Produced Using Microwave Pyrolysis. *ACS Sustain. Chem. Eng.* **2016**, *4*, 930–936. [[CrossRef](#)]